

Nernst and Ettingshausen Effects in Germanium between 300 and 750°K

HERBERT METTE, WOLFGANG W. GÄRTNER, AND CLAIRE LOSCOE

United States Army Signal Research and Development Laboratory, Fort Monmouth, New Jersey

(Received March 6, 1959)

The Nernst and Ettingshausen effects in germanium single crystals of different conductivity type and with various impurity densities have been measured between 300 and 750°K in magnetic fields of 9000 gauss; the Nernst effect also at 2100 gauss. The experimental results are compared with theoretical expressions for the Nernst and Ettingshausen coefficients and with previously reported values for the thermal conductivity, which links the two effects through the Bridgman relationship. The qualitative agreement is very good, quantitative discrepancies are explained in terms of deviations of the sample mobilities from the theoretically assumed pure low-field lattice mobilities and by uncertainties in the numerical values used for the theoretical calculations. A derivation of the Nernst constant in the range of negligible phonon-drag effect is given, based on the analogy between thermo- and photomagnetolectric effects.

I. INTRODUCTION

MEASUREMENTS of the Nernst effect in semiconductors have recently been reported by several authors.¹⁻⁴ These investigations were mostly concerned with the interesting phenomena which occur in the phonon-drag region below room temperature. The experiments described here have been carried out in the temperature range above room temperature where carrier diffusion makes the dominant contribution to the Nernst effect. Together with Hall effect and electrical conductivity measurements it may be used to investigate carrier mobilities. Knowledge of this effect is also of practical interest, e.g., because it always occurs in conjunction with the photomagnetolectric effect due to heating of the illuminated surface, and may falsify the results.

Ettingshausen data on germanium or silicon have to our knowledge not yet been reported in the literature. Assuming the validity of the Bridgman relation, one may use Ettingshausen measurements together with Nernst data to determine the heat conductivity at high temperatures. Since the Ettingshausen effect is always present in Hall effect measurements and may amount to as much as 1 deg/cm, and furthermore may not be removed by reversal of the magnetic field, its knowledge can be used to correct dc Hall data.

II. EXPERIMENTAL TECHNIQUES

Figure 1 shows the apparatus which permits measurement of the Nernst and of the Ettingshausen coefficients on the same crystal from room temperature to 500°C and above. The samples were slabs of germanium of $2 \times 0.7 \times 0.1$ cm³, the ends of which were rhodium plated to obtain good electrical contacts. Each sample was

mounted with high-temperature cement to a round brass block provided with threads, which was put into an oven that controlled the ambient temperature. The oven was placed between the poles of a calibrated magnet. Electrical contacts were made to the ends of the sample to pass the current for the Ettingshausen effect and a heater was mounted on one end of the sample to establish the temperature gradient for the Nernst effect. Four tiny chromel-alumel thermocouples (0.002-in. wire) were cemented to the crystal as temperature probes in such a way as to allow by suitable connection of their leads the measurement of (1) the absolute temperature at each of the four points by comparison with a reference temperature, (2) the longitudinal temperature gradient necessary for the Nernst effect, and (3) the transverse Ettingshausen temperature gradient. Tungsten leads on rhodium plated contacts were mounted between the thermocouples at each side to pick up the Nernst-voltage. The thermocouple emf's were measured by a compensation method using a voltage-sensitive galvanometer as the null instrument. Temperature differences of a millidegree could easily be read and fractions of it estimated.

Nernst effect.—In order to eliminate errors due to thermal emf's at the contacts, all readings were taken by reversing the field at constant magnitude. The

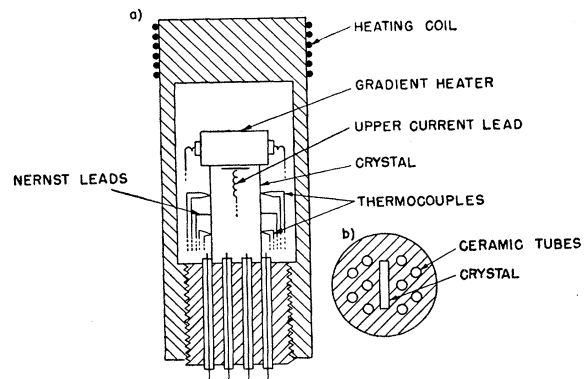


FIG. 1. Apparatus for the simultaneous measurement of TME effects. (a) Cross section; (b) top view of crystal block.

¹Herring, Geballe, and Kunzler, *Phys. Rev.* **111**, 36 (1958).

²T. V. Krylova and I. V. Mochan, *J. Tech. Phys. (U.S.S.R.)* **25**, 2119 (1955).

³R. I. Bashirov and I. M. Tsidi'kovskii, *J. Tech. Phys. (U.S.S.R.)* **26**, 2195 (1956) [translation: *Soviet Phys. (Tech. Phys.)* **1**, 2129 (1956)].

⁴Mochan, Obratsov, and Krylova, *J. Tech. Phys. (U.S.S.R.)* **27**, 242 (1957) [translation: *Soviet Phys. (Tech. Phys.)* **2**, 213 (1957)].

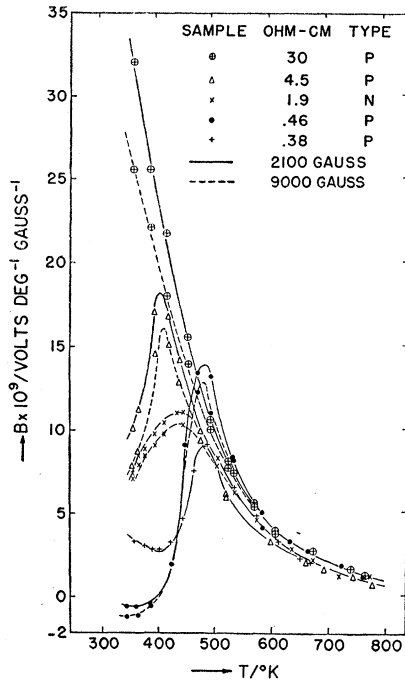


FIG. 2. Experimental Nernst coefficient, B , in n - and p -type germanium of different resistivities, as a function of temperature between 300 and 750°K, measured at 2100 and 9000 gauss.

gradients used were between 2 and 8 deg/cm. No difference was found whether the effect was measured under vacuum or in air. Since preliminary measurements on several samples showed a slight field dependence of B above 3000 gauss over a certain range above room temperature, the Nernst coefficient was determined at two magnetic field strengths, 9000 gauss and 2100 gauss.

Ettingshausen effect.—Since small temperature changes down to several millidegrees had to be measured on an object which itself was at temperatures up to 500°C, it was necessary to obtain these measurements by a lengthy and careful process of repeatedly reversing the magnetic field at intervals of 30 seconds. Then the direction of the current was reversed and the set of measurements repeated at the same temperature. The readings were plotted and averaged graphically thereby eliminating errors due to drifting of the ambient temperature and of the gradient and due to effects which might have been caused by self heating of the sample under the Ettingshausen current or by small gradients within the sample due to irregular heat dissipation from the sample surface. Thirty seconds were found to be enough time to establish temperature equilibrium within the sample after each reversal of field.

In order to obtain a sufficiently large reading accuracy especially in the temperature ranges where the effect is small, all measurements were taken only at fields of 9000 gauss and current densities of 1 to 3 amp/cm².

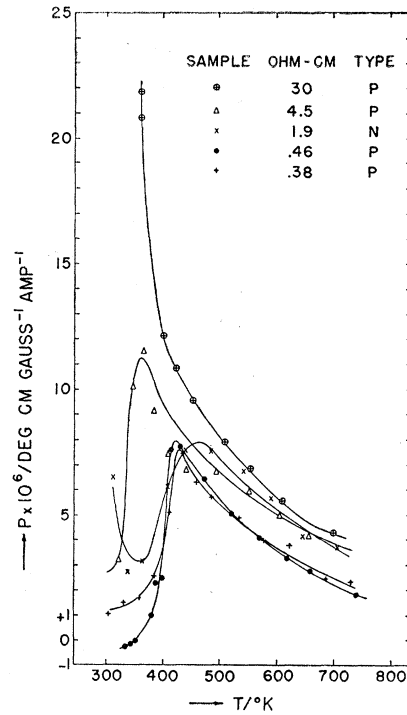


FIG. 3. Experimental Ettingshausen coefficient, P , in n - and p -type germanium of different resistivities, as a function of temperature between 300 and 750°K, measured at 9000 gauss.

Although the effect was linear with the current at least to a measuring accuracy of several percent, as control measurements at its optimal temperatures confirmed, the low-field values are probably slightly higher for temperatures below 150°C in a similar way as in the case of the related Nernst effect.

III. EXPERIMENTAL RESULTS AND INTERPRETATION

Figure 2 shows the measured values for the Nernst effect at two values of magnetic field; Fig. 3 shows the Ettingshausen effect for the same samples at 9000 gauss. In the temperature range between 300 and 600°K the Nernst data by Bashirov and Tsidil'kovskii⁵ when suitably normalized are compatible with our results. One notices that in the lower temperature range a magnetic-field dependence of the Nernst effect is noticeable which decreases towards higher temperatures. Since the Nernst and Ettingshausen coefficients, B and P , are related through the Bridgman relationship⁵

$$BT = \kappa P \quad (1)$$

(where T is the absolute temperature and κ is the thermal conductivity), one may derive the temperature dependence of the thermal conductivity from simultaneous measurements of the two effects. The results of such a calculation are shown in Fig. 4 together

⁵ P. W. Bridgman, Phys. Rev. 24, 644 (1924).

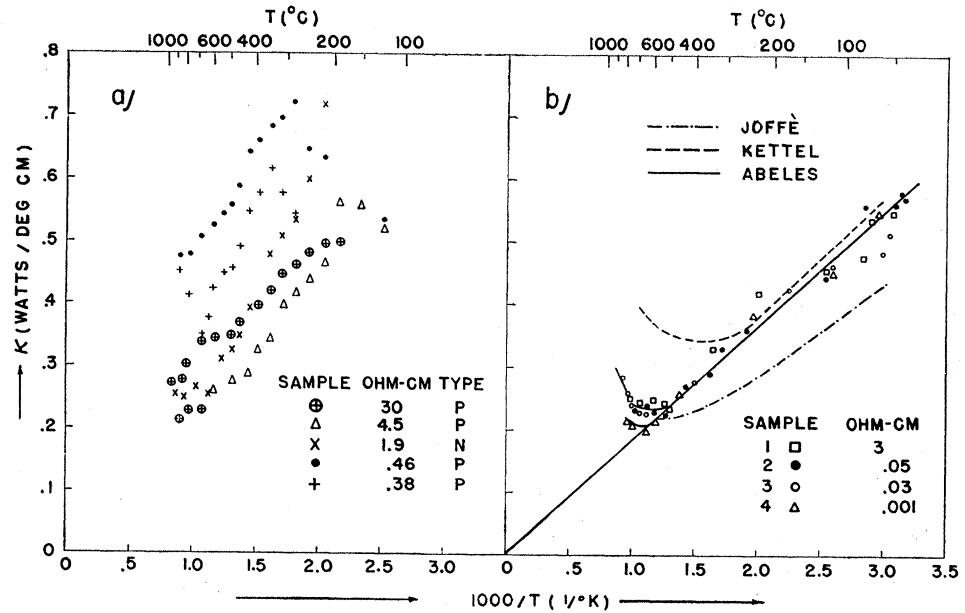


FIG. 4. Heat conductivity of germanium. (a) Calculated from the Nernst and Ettingshausen coefficients, (b) measured by different authors.

with previously reported measurements of the thermal conductivity of germanium.⁶ The quantitative agreement is fairly good for high resistivity samples, but is poorer for low resistivity samples, indicating that our Nernst data may be too high or our Ettingshausen data too low. To compare the experimental results with theoretical expectations, Figs. 5 and 6 show plots of theoretical Nernst and Ettingshausen coefficients as a function of temperature with the impurity content as the parameter. N_d and N_a in Figs. 5 and 6 denote the donor and acceptor densities, respectively. The expression for the Nernst coefficient⁷ due to carrier diffusion alone (assuming mobilities and lifetimes constant),

$$B = \frac{qD(\mu_n^H + \mu_p^H)}{\sigma(n_0 + p_0)} \frac{d(n_i^2)}{dT}, \quad (2)$$

is derived in the Appendix, Eq. (A11), as a special case of a theory for thermomagnetolectric effects which is based on the analogy of these effects and the photomagnetolectric effect.

In Eq. (2), q is the electronic charge; D is the ambipolar diffusivity, $D = D_n(p_0 + n_0)/(p_0 + bn_0)$; D_n is the diffusion constant of electrons in highly p -type material, $D_n = (kT/q)\mu_n^D$; p_0 and n_0 are the equilibrium carrier densities; b is the ratio of electron drift mobility, μ_n^D , over hole drift mobility, μ_p^D , i.e., $b = \mu_n^D/\mu_p^D$; μ_n^H and

μ_p^H are the electron and hole Hall mobilities; n_i is the intrinsic carrier density; σ is the conductivity of the sample, $\sigma = q(\mu_n^D n_0 + \mu_p^D p_0)$.

The following numerical values have been used to obtain Fig. 5:

$$\begin{aligned} n_i^2 &= 3.1 \times 10^{32} \times T^3 \times \exp(-9.101 \times 10^3/T),^8 \\ \mu_n^D &= \mu_n^H = 4.9 \times 10^7 \times 10^{-1.66, 9-11} \\ \mu_p^D &= 1.05 \times 10^9 \times T^{-2.33, 9, 11} \\ \mu_p^H &= 1.8 \mu_p^D.^{12} \end{aligned}$$

Using the Bridgman relationship, Eq. (1), and the expression (2) for the Nernst coefficient, the Ettingshausen coefficient, P , has been calculated and plotted in Fig. 6 employing the following empirical temperature dependence of the thermal conductivity, κ ,

$$\kappa = (181/T) \text{ watts/(deg. cm)}, \quad (3)$$

which is based on the data reported by Abeles⁶ and which are similar to the ones published by Ioffe⁶ and Kettel.⁶ The temperature range of P has been limited to the range over which relationship (3) appears to be valid.

A comparison between the experimental and theoretical curves for the Nernst coefficient in Figs. 2 and 5 shows good qualitative agreement. The theoretical curves lie, in general, higher than the experimental values which may be due to the fact that the theoretically assumed values for the mobilities are probably too high for the samples used. An additional uncertainty

⁶ B. Abeles, Conference on Thermoelectricity sponsored by the U. S. Naval Research Laboratory, Washington, D. C., September 3-4, 1958 (unpublished); and *Proceedings of the International Conference on Semiconductors, Rochester, August, 1958* [J. Phys. Chem. Solids 8, 340 (1959)]; A. F. Ioffe, Can. J. Phys. 34, 1342 (1956); F. Kettel, Münster Meeting of the German Physical Society, April, 1957; and J. Phys. Chem. Solids 10, 52 (1959).

⁷ For a comprehensive list of references on earlier theoretical treatments see reference 1.

⁸ F. J. Morin and J. P. Maita, Phys. Rev. 94, 1525 (1954).

⁹ M. B. Prince, Phys. Rev. 92, 681 (1953).

¹⁰ P. P. Debye and E. M. Conwell, Phys. Rev. 93, 693 (1954).

¹¹ F. J. Morin, Phys. Rev. 93, 62 (1954).

¹² E. M. Conwell, Proc. Inst. Radio Engrs. 46, 1281 (1958).

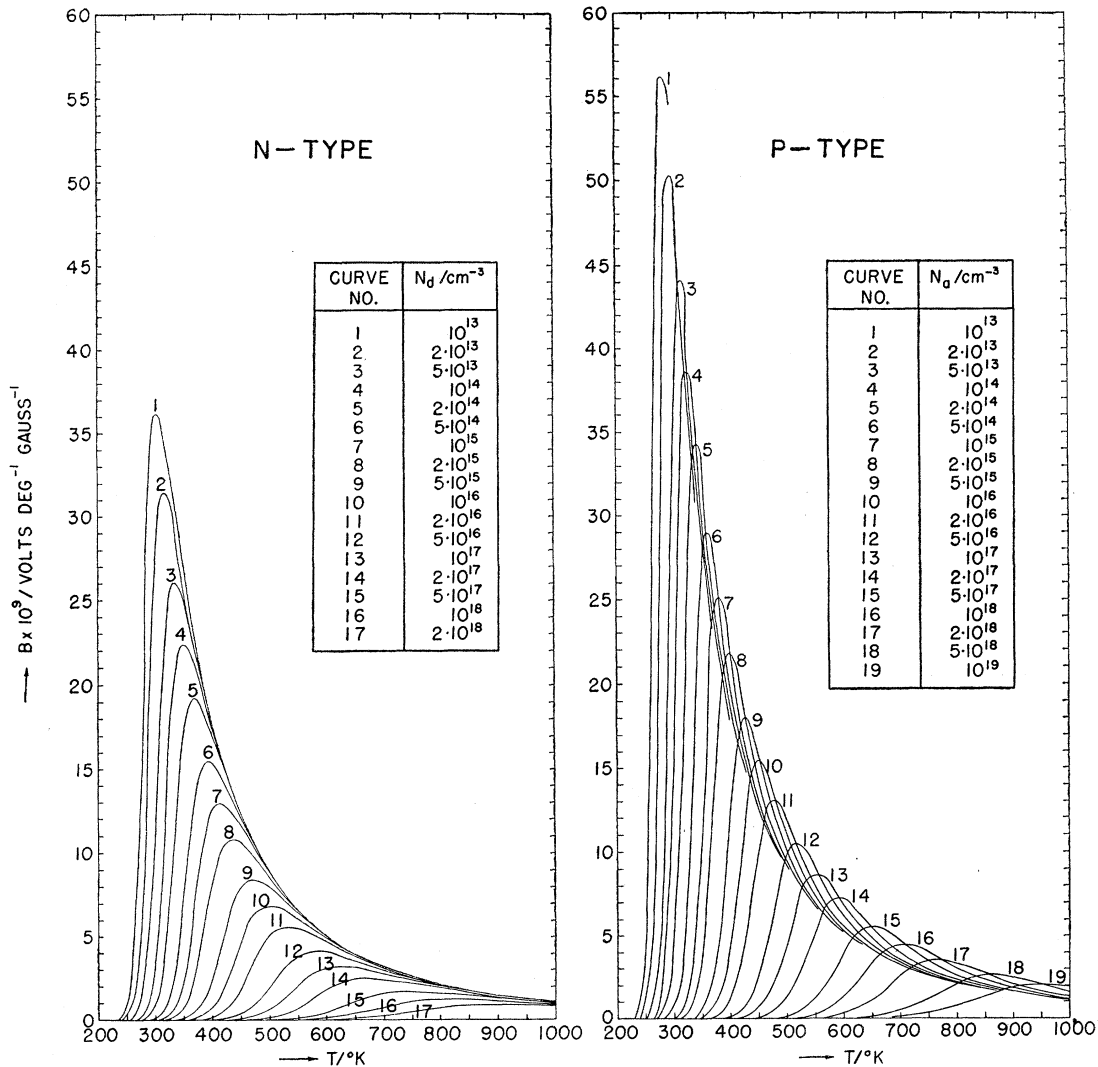


FIG. 5. Theoretical Nernst coefficient, B , in n - and p -type germanium with various impurity concentrations as a function of temperature between 200 and 1000°K.

enters through the assumption made about the ratio between Hall and drift mobilities. To achieve quantitative agreement between theory and experiment, Hall and drift mobilities shall be measured simultaneously with the thermomagnetolectric effects in future experiments.

Since the theoretical Ettingshausen curves, Fig. 6, are derived for zero field but the experimental data are taken at 9000 gauss, no direct comparison is possible. One may, however, assume that the field dependence of the Ettingshausen effect is similar to that demonstrated for the Nernst effect in Fig. 2 so that the true zero-field values should be higher than in Fig. 3. Another source of uncertainty lies in the fact that heat conductivity measurements in germanium are still quite problematic and the results of different authors

show a certain amount of scattering. The error introduced by the use of relationship (3) to obtain the curves of Fig. 6 may therefore be considerable. In view of these difficulties the agreement between Figs. 3 and 6 may be regarded as satisfactory.

ACKNOWLEDGMENTS

The authors would like to thank Mr. J. Standig, United States Army Signal Research and Development Laboratory, for obtaining the solutions to the differential equations and carrying out all numerical computations for the theoretical curves. Critical comments on the manuscript by Mr. W. van Roosbroeck and Dr. C. Herring of Bell Telephone Laboratories are also gratefully acknowledged.

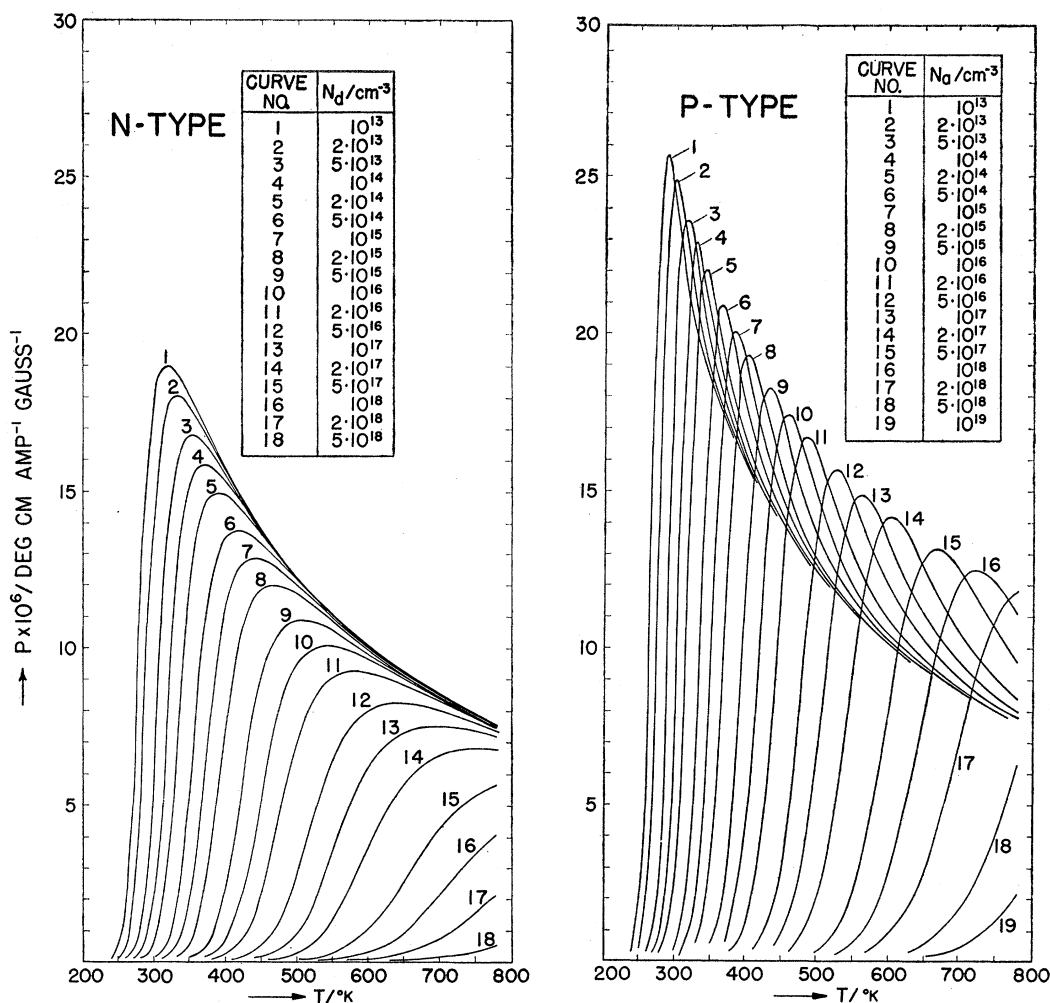


FIG. 6. Theoretical Ettingshausen coefficient, P , in n - and p -type germanium with various impurity concentrations as a function of temperature between 200 and 800°K.

APPENDIX. DERIVATION OF NERNST CURRENTS AND VOLTAGES DUE TO CARRIER DIFFUSION AND FINITE RECOMBINATION

Because of the similarity between the Nernst effect outside the phonon-drag region and the photomagneto-electric (PME) effect,¹³ the phenomenological theory of the spectral distribution of the PME effect¹⁴ is directly applicable¹⁵ if we assume (1) a slab of homogeneous semiconductor material, infinite in the x and z directions; (2) a (weak) magnetic field in the z direction; (3) a temperature gradient in the y direction (isothermal

Nernst effect); (4) local charge neutrality, $p-p_0 = n-n_0$; $\text{grad } n = \text{grad } p$; (5) steady state; (6) short or open-circuit conditions; (7) small Hall angles; (8) small injection levels, so that

$$|p-p_0| \ll \frac{1}{2}(p_0+n_0), \tag{A1}$$

$$|p-p_0| \ll (p_0+bn_0)/(b+1); \tag{A2}$$

(9) negligible phonon-drag and Soret effects; (10) constant mean free time; (11) negligible temperature dependence of the energy gap; (12) the "thermal Hall angles" for carrier transport under the influence of a temperature gradient are negligibly different from the ordinary Hall angles for carrier transport in an electric drift field. These assumptions may be expected to hold in and near the intrinsic range of germanium and silicon.

The minority carrier density is then governed by a

¹³ For a comprehensive list of references and a rigorous formulation of the underlying theory see W. van Roosbroeck, Phys. Rev. **101**, 1713 (1956).

¹⁴ W. Gärtner, Phys. Rev. **105**, 823 (1957).

¹⁵ Under certain assumptions some of the equations in this Appendix may be specialized to agree with relationships given by G. E. Pikus, Zhur. tekhn. Fiz. (U.S.S.R.) **26**, 22 (1956) [translation: Soviet Phys. (Tech. Phys.) **1**, 17 (1956)], in his extensive theoretical discussion of thermomagnetolectric effects including the influence of recombination.

differential equation of the form

$$\frac{d^2 p}{dy^2} - \frac{p - p_0}{L^2} = -\frac{g(y)}{D}. \quad (\text{A3})$$

Equation (A3) applies to holes in n -type material and an analogous relationship holds for electrons in p -type crystals. $p(y)$ is the hole density; L is the diffusion length, defined as $L^2 = D\tau$; τ is the lifetime of excess carriers; $g(y)$ denotes a bulk generation rate due to other influences than temperature (e.g., light) which is a function of y only. It could, e.g., be used to investigate the influence of illumination on the Nernst and Ettingshausen effects or to analyze the contribution of the Nernst effect in a measurement of the photomagnetolectric effect. For the following considerations we set it equal to zero. $p_0(y)$ is the equilibrium hole density corresponding to the temperature at point y , and it is determined from $n_0 - p_0 = N_a - N_d$ and $n_0 p_0 = n_i^2(y)$. The formulation of Eq. (A3) is thus not restricted to the linear approximation for the equilibrium carrier densities used below. Equation (A3) must be solved under the boundary conditions

$$\mathcal{R}_1 + D dp/dy = s_1(p - p_0) \quad \text{at } y=0, \quad (\text{A4a})$$

and

$$\mathcal{R}_2 - D dp/dy = s_2(p - p_0) \quad \text{at } y=w, \quad (\text{A4b})$$

where \mathcal{R}_1 and \mathcal{R}_2 are surface generation rates (e.g., due to light) which are set equal to zero in the following; s_1 and s_2 are the surface recombination velocities at the front and back surface, respectively; w is the thickness of the sample. We now further assume that L is a constant independent of y , and that $p_0(y)$ is given by the linear approximation $p_0(y) = a - by$, where a is the equilibrium carrier concentration corresponding to the temperature at the front surface, $a = p_0(0)$, and $b = -(dp_0/dT)(\text{grad } T)$, where $(\text{grad } T)$ is treated as a constant. The solution of Eq. (A3) for $g(y) = 0$ is then given by

$$p(y) = A e^{y/L} + B e^{-y/L} - by + a, \quad (\text{A5})$$

where

$$A = \frac{DbL[e^{-w/L}(D - s_2L) - (D + s_1L)]}{e^{-w/L}(D - s_1L)(D - s_2L) - e^{w/L}(D + s_1L)(D + s_2L)},$$

and

$$B = \frac{DbL[e^{w/L}(D + s_2L) - (D - s_1L)]}{e^{-w/L}(D - s_1L)(D - s_2L) - e^{w/L}(D + s_1L)(D + s_2L)}.$$

Result (A5) indicates that in thin slabs with different recombination velocities at the two surfaces, the Nernst voltages and currents will have different magnitudes depending on the direction of the temperature gradient. Standig¹⁶ has shown that Eq. (A3) yields an analytical result also for the case where L^2 or $1/L^2$ vary as $c + dy$, i.e., are explicit functions of the temperature across the slab. The solution then contains modified Bessel functions of the first and second kind. The short-circuit Nernst current, $I_x^{(sc)}$, and the open-circuit Nernst field, $E_x^{(oc)}$, are given by Eqs. (21) and (22) in reference 14.

$$I_x^{(sc)} = -qD\theta[p(0) - p(w)], \quad (\text{A6})$$

and

$$E_x^{(oc)} = -I_x^{(sc)}/(\sigma w), \quad (\text{A7})$$

where $\theta = H(\mu_n^H + \mu_p^H)$ is the sum of the Hall angles. These equations hold for the case of small temperature differences and thus small changes in conductivity across the sample. If this condition is not satisfied, Eqs. (37) and (39) of reference 11 must be used.

To obtain an expression for the bulk Nernst constant, we must specialize solution (A5) for the case of infinite surface recombination velocities, ($s_1 = s_2 = \infty$) and negligible volume lifetime, $L = 0$, and we obtain

$$p(0) - p(w) = bw = -\frac{dp_0}{dT}(\text{grad } T)w. \quad (\text{A8})$$

The Nernst constant, B , is defined as $B = E_x^{(oc)}/(\mathbf{H} \cdot \text{grad } T)$. From Eqs. (A6) through (A8) we therefore find

$$B = \frac{qD(\mu_n^H + \mu_p^H)}{\sigma} \frac{dp_0}{dT}. \quad (\text{A9})$$

Since dp_0/dT and $np = n_i^2$ and thus

$$\frac{dp_0}{dT} = \frac{1}{n_0 + p_0} \frac{d(n_i^2)}{dT}, \quad (\text{A10})$$

one obtains

$$B = \frac{qD(\mu_n^H + \mu_p^H)}{\sigma(n_0 + p_0)} \frac{d(n_i^2)}{dT}. \quad (\text{A11})$$

This last expression has been used to calculate the theoretical curves of Fig. 5.

¹⁶ J. Standig (private communication).